Hydrodynamic Characteristics of a Gas-Liquid-Solid Fluidized Bed Containing a Binary Mixture of Particles

Hydrodynamic characteristics were investigated in a cocurrent gas-liquid-solid fluidized bed containing a binary mixture of particles. The binary mixtures used were ten combinations of eight types of spherical particles differing in diameter and/or density. The density variation of the particles in the mixture was found to exhibit a stronger effect on the extent of solids mixing or segregation than did the size variation of the particles in the mixture. Additionally, a solids layer inversion phenomenon was found to occur in a bed of small, heavy alumina beads and large, lighter glass beads. The minimum fluidization velocity of binary mixtures correlated well empirically with the superficial gas velocity, weight fraction of jetsam particles, and particle terminal velocities of jetsam and flotsam particles. Bed expansion and gas holdup for a binary mixture were analyzed for three solids mixing states, namely, complete segregation, partial intermixing, and complete intermixing. The analysis indicates that the serial model, or segregation model, predicts the bed voidage satisfactorily even when the bed is at the complete intermixing state.

LIANG-SHIH FAN, AKINORA MATSUURA and SONG-HSING CHERN

Department of Chemical Engineering
The Ohio State University
Columbus, OH 43210

SCOPE

Gas-liquid-solid fluidized beds have been fully developed and demonstrated in processing technology; as three-phase reactors, they have been employed in the H-oil process for hydrogenation and hydrodesulfurization of residual oil, the H-coal process for coal liquefaction, and the biooxidation process for waste water treatment. In these reactors, a size and/or density distribution of solid particles in the bed is commonly encountered. Particle stratification, or segregation, would occur in the reactors should adequate mixing among particles not be established. Furthermore, mass and heat transfer properties of a gas-liquid-solid fluidized bed with mixed size and/or density particles would deviate from those of a fluidized bed with uniform size and density particles.

Very limited information is available in the literature regarding fundamental characteristics of three-phase fluidized beds with mixed size and/or density particles. Evstropeva et al. (1972) investigated motions of light and heavy particles mainly under a gas-supported fluidization condition and analyzed their experimental results based on a statistical concept. M. N. Epstein et al. (1981) examined the onset of incipient stratification or mixing of particles for liquid-liquid and liquid-solid particle mixtures in a bed which was operated with a stationary liquid and agitated by gas bubbles. They viewed the incipient stratification or mixing process as a quasistatic balance of body forces. Based on visual observation for a gas-liquid-solid fluidized bed containing a binary mixture of glass beads, Fan et al. (1984) noted that there exists a strong correlation between the solids mixing and flow regimes.

In this study experiments were performed to examine the hydrodynamic characteristics of a gas-liquid-solid fluidized bed containing a binary mixture of particles. Analyses were made in connection with the solids mixing behavior in the bed.

CONCLUSIONS AND SIGNIFICANCE

Ten types of binary mixtures of particles differing in diameter and/or density were utilized in this study to examine solids mixing and hydrodynamic characteristics including flow regime, minimum fluidization velocity, bed expansion (or bed voidage), and gas holdup in a cocurrent gas-liquid-solid fluidized bed. The experiments were conducted in a circular plexiglas column of 76.2 mm I.D. The minimum fluidization velocity, bed expansion, and gas holdup for binary mixtures were empirically correlated by utilizing the relationships of those for beds of monocomponent particles.

Flow regime and solids mixing are strongly affected by par-

Correspondence concerning this paper should be addressed to Liang-Shih Fan.

ticle properties. The superficial liquid velocity demarcating the dispersed and coalesced bubble flow regimes for monocomponent particles increases and then decreases with an increase in the particle terminal velocity. The solids mixing state is much more sensitive to variations in particle density than to variations in particle size. Additionally, the solids layer inversion phenomenon may occur in a fluidized bed of a binary mixture containing small, heavy particles and large, lighter particles.

Adding small (or light) particles to large (or heavy) particles reduces the minimum fluidization velocity to a certain extent, depending on the gas velocity. The minimum fluidization velocity in a binary mixture can be correlated in terms of the superficial gas velocity, the weight fraction of jetsam particles, and the particle terminal velocities of jetsam and flotsam particles. The bed expansion (or bed voidage) and gas holdup in a binary mixture can be described for a given solids mixing state by the serial model or the averaging model. The serial model was shown to represent the bed expansion well even when the bed is at the complete intermixing state.

INTRODUCTION

In practical applications of gas-liquid-solid fluidized beds, a size and/or density distribution of solid particles in the bed is commonly encountered. For example, a nonuniformity of particle sizes exists among catalyst particles in catalytic processings, or among solid reactant particles in noncatalytic reactors. Due to uneven growth of biological film on particle surfaces, distributions of particle size and/or density occur during the operation of a fluidized bed bioreactor. Under these circumstances stratification, or segregation, of particles readily occurs, leading to operational complexity for the reactor. Furthermore, characteristics of mass and heat transfer in a gas-liquid-solid fluidized bed with mixed size and/or density particles deviate from those with particles of uniform size and density.

Studies of fundamental behavior in a fluidized bed of mixed size and/or density particles have been limited to gas-solid systems (e.g., Rowe et al., 1972; Chen and Keairns, 1975, 1978; Nienow et al., 1978; Yoshida et al., 1980; Yang and Keairns, 1982) and liquid-solid systems (e.g., Hoffman et al., 1960; Wen and Yu, 1966; Finkelstein et al., 1971; Wen and Fan, 1975; Al-Dibouni and Garside, 1979; Moritomi et al., 1982). Notably, Rowe et al. (1972) investigated particle segregation in gas-solid fluidized beds of binary mixtures of nearly spherical particles and found that a slight difference in particle density readily leads to segregation, while binary mixtures with particle diameter ratios up to 8 are well mixed under almost all conditions. Rowe et al. concluded that particle segregation is proportional to the parameters, $(\rho_H/\rho_L)^{2.5}$ and $(d_B/d_S)^{0.2}$, where ρ_H and ρ_L are densities of heavy and light particles, respectively, and d_B and d_S are diameters of large and small particles, respectively. In contrast, a liquid-solid fluidized bed containing a binary mixture of particles segregates when the particle diameter ratio exceeds 1.3 (Wen and Yu, 1966). However, very little information is available in the literature regarding fundamental characteristics in gas-liquid-solid fluidized beds containing mixed size and/or density particles.

Evstropeva et al. (1972) investigated experimentally the motions of glass particles and polystyrene particles mainly under a gas-supported fluidization condition. Glass beads used were 2.5 mm and 3.9 mm; polystyrene particles were 2.5 mm and 3.9 mm with a density on the order of 1.00 g/cm^3. Colored glass beads and polystyrene particles were used as tracers to simulate the motions of fluidized particles and liquid, respectively. A statistical analysis was performed to account for the motion of the fluidized bed particles and polystyrene particles. M. N. Epstein et al. (1981) defined a criterion for the onset of stratification for liquid-liquid and liquid-solid particle mixtures in a bed operated with a stationary liquid and agitated by gas bubbles. They viewed the incipient mixing or stratification process as a quasistatic balance of body forces. Recently, visual observation was conducted by Fan et al. (1984) to examine solids mixing in a cocurrent gas-liquid-solid fluidized bed containing a binary mixture of particles including 3 mm and 4 mm glass beads and a bed mixture of 3 mm and 6 mm glass beads. They noted that for these binary mixtures: the complete segregation state occurs solely in the dispersed bubble flow regime; the partial intermixing state occurs largely in the dispersed bubble flow and transition regimes and slightly in the coalesced bubble flow regime; and the complete intermixing state occurs largely in the coalesced bubble and slug flow regimes and slightly in the transition regime. Using particles smaller than those of Fan et al. (1984), Sinha et al. (1984) examined the effect of polydispersity of solids on bed stratification, bed expansion and bed contraction for a three phase fluidized bed. They correlated the porosity as a function of four dimensionless groups in which the median diameter was employed to characterize the particle property. They also reported the bed contraction behavior which is similar to that observed for monocomponent systems.

In this study, experiments were conducted to examine the hydrodynamic behavior—i.e., minimum fluidization, bed expansion, and gas holdup—in connection with solids mixing and flow regimes in a gas-liquid-solid fluidized bed of a binary mixture of particles. Ten binary mixtures involving eight types of particles were considered in the study. Empirical or semiempirical correlations were developed to quantify the behavior. Moreover, partial generalization of the flow regime map is attempted for monocomponent particle systems.

EXPERIMENTAL

A schematic diagram of the experimental apparatus is shown in Figure 1. The vertical Plexiglas column is 76.2 mm I.D. with a 2.73 m height. The column consists of three sections, the gas-liquid distributor section, the test section, and the gas-liquid disengagement section. The gas-liquid distributor located at the bottom of the test section was designed in such a manner that uniform distribution of gas and liquid can be maintained in the column. Details of the gas-liquid distributor are given elsewhere (Fan et al., 1982).

Water and air were used as the liquid and gas phases in the experiments. The gas-liquid flow is cocurrent and upward. Pressure taps, which are connected to water manometers, are axially spaced at 51 mm intervals on the column wall of the test section and are used to measure the static pressure gradient along the column.

In each experiment two types of particles that differ in size and/or density were used. The physical properties of particles used in this study are shown in Table 1. The binary mixture systems studied are summarized in Table 2. The particles are all spherical or near spherical. They include both nonporous and porous particles. Porous particle density, i.e., wet density, was measured with specific gravity bottles under the same condition as in the bed. The effect of component weight fraction in a binary mixture on hydrodynamic behavior was studied only for mixtures I through IV.

Flow regimes are classified based on visual observation in the same manner as that of Muroyama et al. (1978). Solids mixing states are also classified based on visual observation in the same manner as that of Fan et al. (1984). Transparent particles are painted different colors to facilitate visual observation.

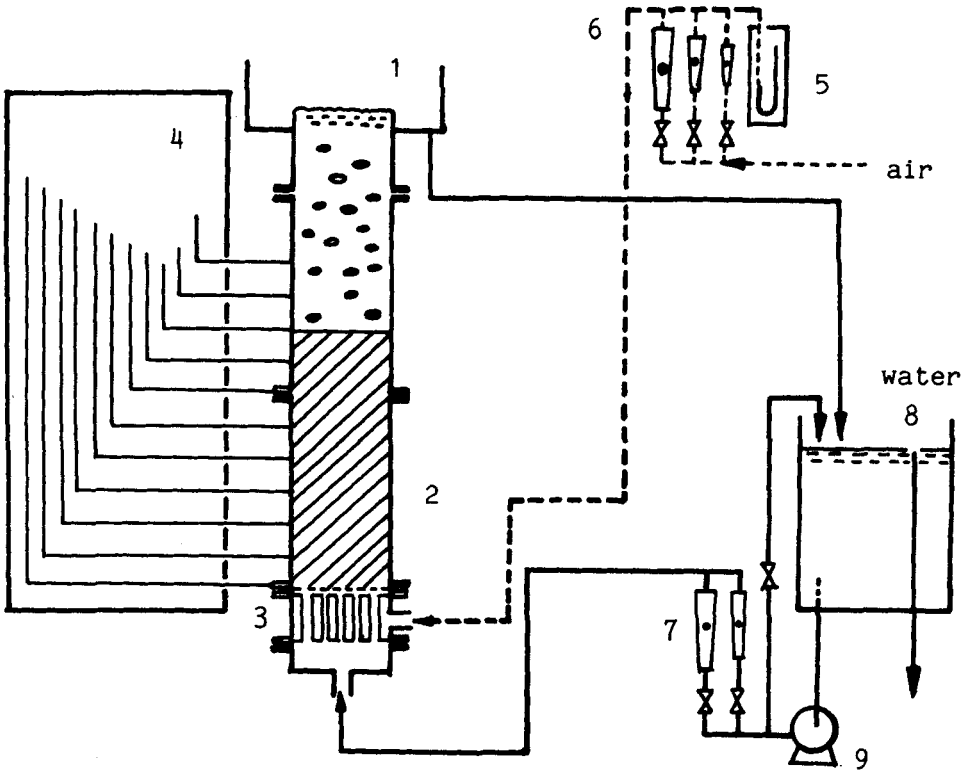

Figure 1. Schematic diagram of experimental apparatus.

1	Gas-liquid disengagement section	5	Pressure gauge
2	Test section	6,7	Rotameters
3	Gas-liquid distributor section	8	Liquid reservoir
4	Manometers	9	Liquid pump

Holdup of individual phases can be obtained indirectly from the experimentally measured static pressure gradient $(-dP/dz)$ and the expanded bed height H, based on the following relationships:

$$\epsilon_s = (W_1/\rho_{s1} + W_2/\rho_{s2})/AH \tag{1}$$

$$-\frac{dP}{dz} = (\epsilon_g\rho_g + \epsilon_\ell\rho_\ell + \frac{W_1 + W_2}{AH})g \tag{2}$$

$$\epsilon_g + \epsilon_\ell + \epsilon_s = 1 \tag{3}$$

RESULTS AND DISCUSSION

Flow Regime

In a gas-liquid-solid fluidized bed, flow regime has a strong effect on the bed expansion behavior and the distribution of the in-bed bubble properties, including bubble rise velocity and bubble size (Matsuura and Fan, 1984). The flow regimes also influence solids mixing states (Fan et al., 1984). The flow regime depends to a great extent on particle properties.

Four flow regimes can be visually identified in a gas-liquid-solid fluidized bed of monocomponent particles. They are:

1. Dispersed bubble flow, representing the flow pattern of small bubbles practically uniform in size.
2. Coalesced bubble flow, representing the presence of the spherical caps or spheroidal bubbles of various sizes.
3. Slug flow, representing the flow pattern of large slugs, whose vertical length is greater than or close to the column diameter.
4. Transition regime, largely located between the dispersed bubble and slug flow regimes.

TABLE 1. PHYSICAL PROPERTIES OF PARTICLES UTILIZED IN THIS STUDY

Particle Notation	Type of Particles	d_p mm	ρ_s g/cm^3	U_t cm/s	$(U_{mf})_{M0}$ cm/s	U_e cm/s	n
P1	Nylon beads	2.50	1.15	7.92	0.58	5.90	2.95
P2	Activated carbon beads	1.74	1.28*	8.62	0.51	7.00	3.13
P3	Glass beads	1.00	2.87	17.0	1.02	16.2	3.10
P4	Glass beads	3.04	2.52	37.5	3.42	24.8	2.43
P5	Glass beads	3.99	2.53	42.9	4.30	30.1	2.47
P6	Glass beads	6.11	2.20	47.7	5.01	34.2	2.31
P7	Alumina beads	2.27	3.69*	42.0	3.36	26.8	2.40
P8	Alumina beads	5.50	3.69*	69.5	7.20	49.6	2.47

* Wet density measured at the same condition as in the bed.

TABLE 2. DESCRIPTION OF BINARY MIXTURE OF PARTICLES CONSIDERED IN THIS STUDY

Mixture Notation	Description*	Weight Ratio 1/2	Diameter Ratio Large/ Small	Density Ratio Heavy/ Light	U_t Ratio Large/ Small
Ia	P4 and P5	1:3	1.33	1.02	1.14
Ib		1:1			
Ic		3:1			
IIa	P4 and P6	1:3	2.00	1.15	1.27
IIb		1:1			
IIc		3:1			
IIIa	P4 and P8	1:3	1.83	1.48	1.85
IIIb		1:1			
IIIc		3:1			
IVa	P6 and P8	1:3	1.09	1.70	1.46
IVb		1:1			
IVc		3:1			
V	P3 and P4	1:1	3.00	1.14	2.21
VI	P1 and P3	1:3.9	2.50	2.50	2.15
VII	P1 and P2	1:1	1.47	1.11	1.09
VIII	P4 and P7	1:1	1.36	1.46	1.12
IX	P4 and P7	1:1.3	1.82	1.49	1.02
X	P6 and P7	3:1	2.69	1.68	1.14

* Particle notation listed in Table 1.

The pattern of the flow regime relationship with the gas and liquid velocities for a monocomponent system was examined for each of the eight particles employed in this study. It was found that for a given fluidized bed there is a strong correlation between the particle terminal velocity in the liquid-phase, U_t, and the superficial liquid velocity demarcating the coalesced bubble flow regime and dispersed bubble flow regime, $(U_\ell)_{dc}$. Figure 2 shows such a relationship. As U_t is increased, the value of $(U_\ell)_{dc}$ increases, reaches a maximum at U_t equal to 34.3 cm/s, and then decreases. The variation of $(U_\ell)_{dc}$ with U_t can be expressed by the following equations:

$$(U_\ell)_{dc} = 0.0696U_t^{1.50} \text{ for } U_t \leq 34.3 \text{ cm/s} \quad (4)$$

$$(U_\ell)_{dc} = 5.72 \times 10^3 U_t^{-1.70} \text{ for } U_t \geq 34.3 \text{ cm/s} \quad (5)$$

A particle terminal velocity of 34.3 cm/s corresponds, for example, to the terminal velocity in water of 2.55 mm glass beads with a density of 2.52 g/cm^3. N. Epstein (1983) reported that a three-phase fluidized bed containing sand particles of greater than 3 mm tends to be in the dispersed bubble flow regime, while that of less than 3 mm tends to be in the coalesced bubble flow regime. It is noted that the diameter of sand particles Epstein reported is very close to that corresponding to U_t of 34.4 cm/s. However, the present study shows that, as indicated earlier, the demarcation between the coalesced bubble flow regime and the dispersed bubble flow regime strongly depends on the liquid velocity used in the system.

The operating range of a fluidized bed is constrained by the operating limits of a fixed bed and a transport bed. Figure 2 shows the transition velocity for the liquid from fluidized bed operation to transport bed operation at $U_g = 0$. The liquid velocity under this transition condition is equivalent to U_t. The transition velocity for the liquid from fixed bed operation to fluidized bed operation corresponds to the minimum fluidization velocity. Figure 2 shows the minimum fluidization velocity for $U_g = 15$ cm/s calculated based on Eq. 7 for several specific particles; this will be discussed later.

As noted by Fan et al. (1984), four different flow regimes were also observed in a fluidized bed of a binary mixture of large glass beads. This study confirms that a similar pattern for flow regimes also exists in other binary mixtures of particles of substantial difference in size and/or density. Figures 3 and 4 show representative flow regime maps for mixtures IVb and X, respectively. It is seen that particle properties have profound effects on the flow regime maps. It is noted, however, that for all mixtures, the gas velocity exhibits negligible effects on the liquid velocity demarcating the

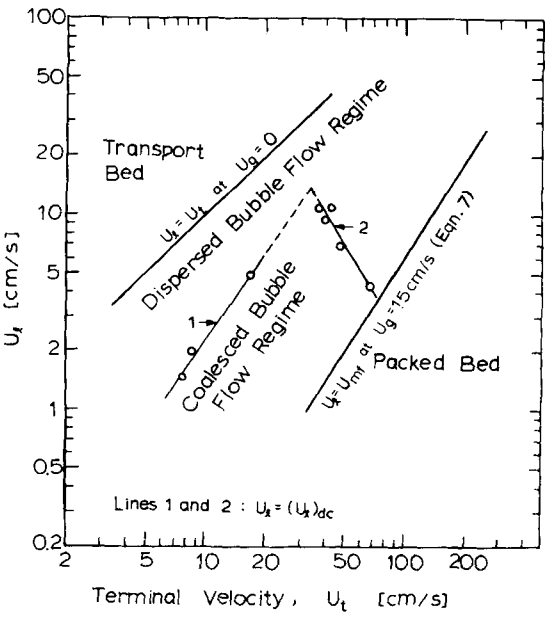

Figure 2. Relationship between particle terminal velocity and superficial liquid velocity, demarcating coalesced and dispersed bubble flow regimes for monocomponent systems.

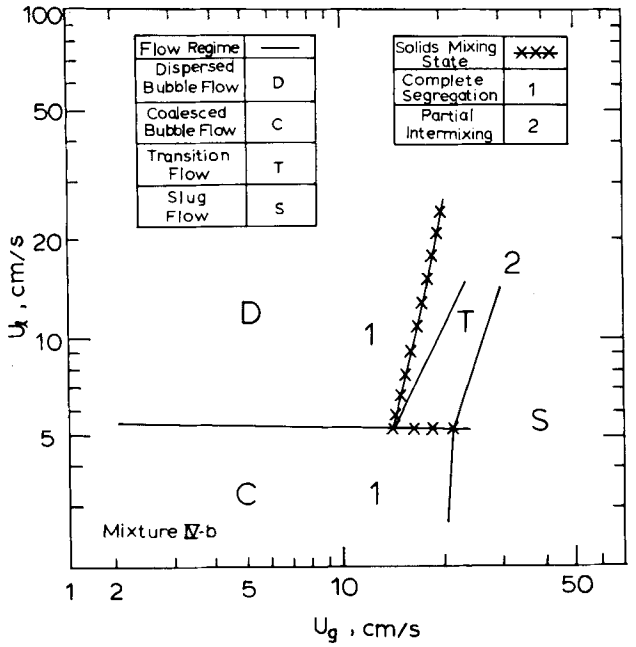

Figure 3. Maps for flow regime and solids mixing state for binary mixture IVb.

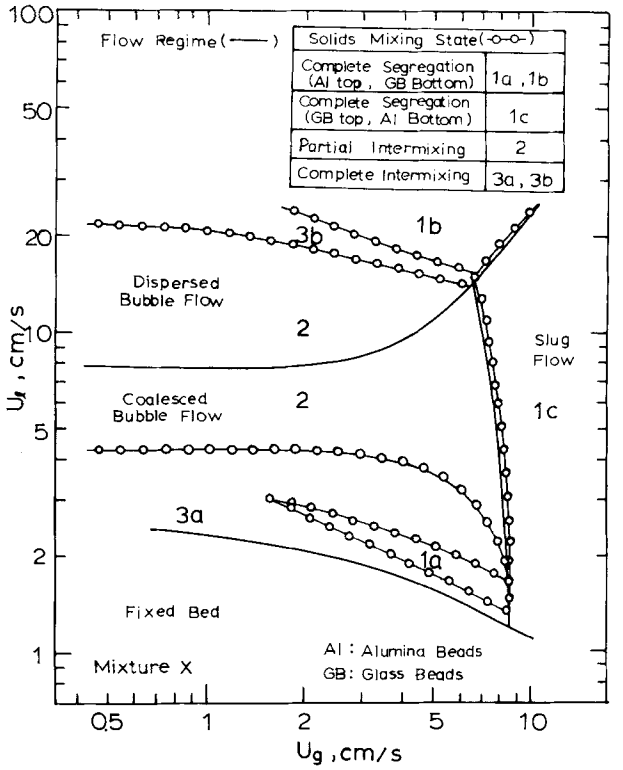

Figure 4. Maps for flow regime and solids mixing state for binary mixture X.

dispersed bubble flow regime and coalesced bubble flow regime, as observed for the monocomponent systems. On the other hand, the demarcation between the coalesced bubble flow regime and slug flow regime is strongly affected by gas velocity and only slightly affected by liquid velocity. For a binary mixture with large particles as one component or both components, slug flow occurs at a relatively high gas velocity as evidenced in these figures. Bubble disintegration caused by the presence of heavy alumina beads is distinct for a binary mixture, for example, mixture IV. A similar phenomenon for bubble disintegration induced by heavy particles was observed by Ostergaard (1969) and Lee et al. (1974) for monocomponent systems.

Solids Mixing States

Solids mixing in a gas-solid fluidized bed is characterized by axial mixing, wake phase and bulk phase exchange, segregation, and bulk circulation promoted by bubbles (Gibilaro and Rowe, 1974). Solids mixing in a liquid-solid fluidized bed is characterized by particle settling due to variation of the bulk density in the bed and particle random movement. Solids mixing in a gas-liquid-solid fluidized bed possesses the characteristics of those of the gas-solid fluidized bed and liquid-solid fluidized bed. Thus it is extremely difficult to analyze the fundamental behavior of solids mixing in a gas-liquid-solid fluidized bed. The analysis, however, can be eased with the knowledge of the flow regime of the system.

Figure 3 shows the solids mixing and flow regime maps for mixture IVb consisting of glass beads and alumina with a diameter ratio of 1.11. It is seen that the complete intermixing state is not achieved for mixture IVb over the four flow regimes considered. The particles segregate even at high gas velocities. Similar solids mixing and flow regime behavior were observed for mixture III consisting of alumina beads (5.5 mm) and glass beads (3.0 mm) with a density ratio of 1.46. For mixtures III and IV, the correlation between the solids mixing map and flow regime map is less prominent than that for mixtures I and II, in which complete intermixing was observed to occur largely in the coalesced bubble flow regime and slug flow regime and slightly in the transition regime.

Figure 4 shows the solids mixing states for mixture X, which consists of small, heavy alumina beads of 2.2 mm dia. and large, light 6.0 mm glass beads. In this case, solid mixing states are much more complicated than other mixtures due to complex relative bed density variations with gas and liquid velocities for monocomponent beds of mixture X particles. Specifically, solids layer inversion was observed in the gas-liquid-solid fluidized bed, and complete intermixing states were seen in two different regions, designated 3a and 3b in Figure 4. At a constant gas velocity of 5 cm/s, the bed was observed to exhibit various solids mixing states with increasing liquid velocity. Specifically, the minimum fluidization condition was observed at liquid velocity of 1.7 cm/s. Near the minimum fluidization velocity solids mixing is in the complete intermixing state (region 3a). Between liquid velocities of 1.9 and 2.1 cm/s the small, heavy alumina beads only were observed near the upper portion of the bed while large, lighter glass beads were of the majority in the lower portion (region 1a). As liquid velocity increased further between 2.1 and 3.7 cm/s, the complete intermixing state 3a was seen again. Between liquid velocities of 3.7 and 16 cm/s, an alumina bead-rich layer was observed near the bottom and a glass bead-rich layer was observed near the surface of the bed (region 2). Note that this region straddles the flow regime boundary between dispersed bubble flow and coalesced bubble flow regimes. Partial intermixing takes place in the middle of the bed. The partial intermixing portion of the bed decreases in size with increasing liquid velocity. Under conditions of liquid velocity between 16 and 19 cm/s, alumina and glass beads are once more completely mixed throughout the entire bed (region 3b). Beyond a liquid velocity of 19 cm/s, an alumina bead layer is observed at the top of the bed while a glass bead layer is seen in the lower portion (region 1b). The boundary between alumina and glass beads is quite distinct. Solids mixing at this condition is in the complete segregation state.

It is interesting to note that these complicated solids mixing states were observed only in the coalesced bubble flow and dispersed

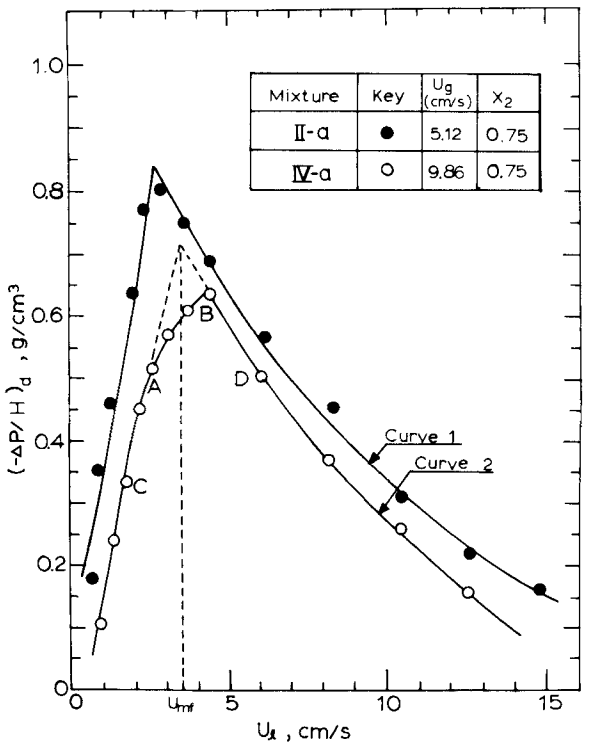

Figure 5. Determination of U_{mf} for mixtures IIa and IVa.

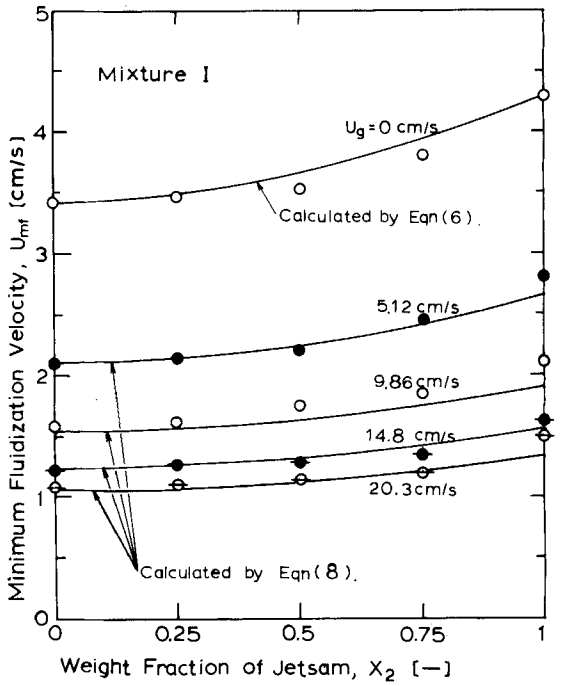

Figure 6. Variation of U_{mf} with X_2 as a function of U_g for mixture I.

bubble flow regimes. In the slug flow regime, only the complete segregation state (region 1c) was observed, with alumina beads at the bottom and glass beads at the top, i.e., an "inverted solids layer" of region 1a or 1b. Note that at gas velocities less than 1.5 cm/s the solids mixing state designated 1a in Figure 4 was not observed.

For mixtures VI, VIII, and IX, the solids mixing states are reflected by the flow regimes in the gas-liquid-solid fluidized beds. The complete intermixing of particles occurs only in the slug flow regime for these mixtures. The complete segregation of particles occurs only at very high liquid velocities in the dispersed bubble flow regime. In the coalesced bubble flow regime and over a wide range of the dispersed bubble flow regime, two distinguishable regions are observed in the bed: the upper region of the bed consists of only flotsam particles, while the lower region of the bed consists of a nearly uniform mixture of jetsam and flotsam particles. Only the complete intermixing state is observed in the gas-liquid-solid fluidized bed containing mixture VII. Obviously, bubble movement establishes a dominating driving force for solids mixing in this binary system.

It is evident that the extent of solids mixing is more sensitive to particle density variations than to particle diameter variations. For example, solids mixing maps were observed to be similar for mixtures I, II, and V, which have the same particle density but with particle diameter ratios (large/small) ranging from 1.31 to as large as 3.04. Mixtures II and III, and V and VI, having nearly equal diameter ratios for the particles in the mixture, but different density ratios, show a distinct difference in the solids mixing maps. It is interesting to note that mixtures I and X have the same U_t ratios, but exhibit entirely different solids mixing behavior due to the relative differences in density and size of particles in these mixtures.

The effect of the weight ratio of binary mixture particles on the solids mixing map and flow regime map was investigated for mixtures I through IV. It was found that the weight ratio of particles (1 to 3, 1 to 1, and 3 to 1) has negligible effects on the solids mixing map and flow regime map for these mixtures.

Minimum Fluidization Velocity

The minimum fluidization velocity in this study was obtained from the relationship between pressure gradient and superficial liquid velocity. For a binary mixture in gas-liquid-solid fluidization at the minimum fluidization condition, the pressure gradient-superficial liquid velocity relationship is affected by the state of intermixing or segregation of particles. The minimum fluidization for two extremes of solid mixing states, i.e., complete intermixing and complete segregation, are analyzed for the weight ratio of flotsam to jetsam of 1:3 as shown in Figure 5. The solids mixing for mixtures IIa and IVa at the minimum fluidization condition is in states of complete intermixing and complete segregation, respectively. Because of considerable particle reorientation from the premixing state, the minimum fluidization velocity determined from the decreasing liquid velocity is not identical to that from the ascending liquid velocity for a solids mixing state of complete segregation or partial intermixing at the minimum fluidization condition. Thus, the minimum fluidization velocity reported in this study is determined only by the ascending liquid velocity. Details are given in the following.

As shown by curve 1 of Figure 5, mixture IIa exhibits a clear break point at the minimum fluidization condition with the gas velocity set at 5.12 cm/s. The solids mixing map reported by Fan et al. (1984) indicates that for this binary mixture at the given gas velocity of 5.12 cm/s, the complete intermixing of solid particles can be reached at liquid velocities up to 8.0 cm/s. The state of solids mixing over the range of the liquid velocity required to obtain the pressure gradient vs. superficial liquid velocity plot for determining the minimum fluidization velocity is in the state of complete intermixing. Thus, the pressure gradient-superficial liquid velocity relationship is expected to be similar to that for the system of uniform particle properties. The decrease in $(-\Delta P/H)_d$ as the liquid velocity increases beyond U_{mf} is due to the increase of the expanded bed height.

In contrast, in curve 2 of Figure 5 mixture IVa exhibits a gradual decrease in the rate of $(-\Delta P/H)_d$ variation with the liquid velocity. It is interesting to note that points A and B on curve 2 in the figure, corresponding to the beginning and end of the curvature around

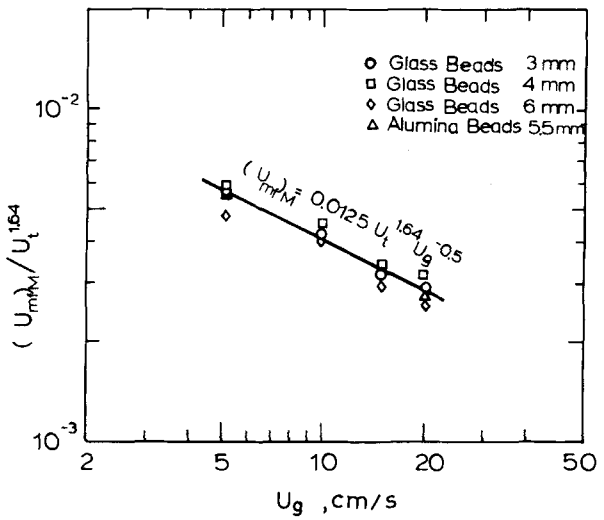

Figure 7. Correlation for the minimum fluidization velocity for monocomponent systems of large particles.

the minimum fluidization point, are very close to the minimum fluidization velocity for the flotsam particles, $(U_{mf})_1$, and that for the jetsam particles, $(U_{mf})_2$, respectively. As the liquid velocity increases to close to $(U_{mf})_1$ for a well-mixed bed at the gas velocity of 9.86 cm/s, some flotsam particles migrate from the mixture to the top of the packed bed. As the liquid velocity further increases toward $(U_{mf})_2$, more flotsam particles separate from the packed bed and fluidize. The bed in this condition exhibits a coexistence of a fluidized region consisting mainly of flotsam particles and a packed region consisting mainly of jetsam particles. The gradual decrease in the rate of $(-\Delta P/H)_d$ variation with the liquid velocity reflects the continuous separation of the two types of particles over the range from $(U_{mf})_1$ to $(U_{mf})_2$. As the liquid velocity increases beyond $(U_{mf})_2$, the entire bed fluidizes, leading to a sharp decrease in $(-\Delta P/H)_d$. U_{mf} of the mixture in this condition is obtained by extrapolating CA and DB as shown in the figure. Indeed, the state of solids mixing around the minimum fluidization point for mixture IV is complete segregation, as given in Figure 3.

Figure 6 shows the minimum fluidization velocities for mixture I with three different weight fractions of jetsam particles as well as monocomponent jetsam or flotsam particles. It is seen that the effect of the weight fraction of the jetsam particles, X_2, on U_{mf} decreases as gas velocity increases. Furthermore, U_{mf} can be correlated in terms of $(U_{mf})_1$, $(U_{mf})_2$, and X_2 by

$$\frac{U_{mf}}{(U_{mf})_1} = \left[\frac{(U_{mf})_2}{(U_{mf})_1}\right]^{X_2^{1.69}} \tag{6}$$

In arriving at Eq. 6 experimental values for $(U_{mf})_i$ are used. It is noted that Eq. 6 also fits well with some of the other mixtures tested, e.g., mixtures II through IV. Naturally, to employ Eq. 6 for prediction of U_{mf} for a binary mixture of particles, accurate account of $(U_{mf})_i$ is necessary. For example, for glass beads of 3 (3.04), 4 (3.99), and 6 (6.11) mm, and alumina beads of 5.5 mm, Figure 7 shows the minimum fluidization velocity for the gas velocity ranging from 5 to 20 cm/s and its correlation equation:

$$(U_{mf})_M = 0.0125 U_g^{-0.5} U_t^{1.64} \tag{7}$$

Equation 7 is valid for $5 \le U_g \le 20$ cm/s and $38 \le U_t \le 70$ cm/s. The results given by Eq. 7 deviate slightly from the empirical correlation for the minimum fluidization velocity for monocomponent beds of coarse/large particles proposed by Begovich and Watson (1978). More work is needed for generalization of the correlation for minimum fluidization velocity for monocomponent systems. Thus, combining Eqs. 6 and 7 yields the minimum fluidization velocity for a binary mixture of particles including glass beads (3, 4, and 6 mm) and alumina beads (5.5 mm), i.e., mixtures I through IV as given in the following:

$$U_{mf} = 0.0125 U_g^{-0.5} U_{t1}^{1.64} \left(\frac{U_{t2}}{U_{t1}}\right)^{1.64 X_2^{1.69}} \tag{8}$$

The predicted values for minimum fluidization velocity for gas-liquid-solid systems based on Eq. 8 are plotted in Figure 6, for mixture I. It is seen from the figure that the predictions is in good agreement with the experimental data.

Bed Expansion and Gas Holdup

Bed expansion and gas holdup in a fluidized bed of a binary mixture of particles can be analyzed for three solids mixing states, namely, complete segregation state, complete intermixing state, and partial intermixing state. The prediction of bed expansion and gas holdup for a binary mixture system can readily be made based on that for a monocomponent system. Thus, the accuracy of the prediction of bed expansion and gas holdup for a binary mixture system strongly hinges on that for a monocomponent system. Correlations for bed expansion and gas holdup for monocomponent systems consisting of various particles used in the present study were recently reviewed by Muroyama and Fan (1985). In the following, a general approach for estimating bed expansion and gas holdup for a binary system using these correlations is illustrated by a specific application to mixtures I and II.

Monocomponent System

Chern et al. (1984) recently investigated bed expansion and gas holdup characteristics in a three-phase fluidized bed using 3, 4, and 6 mm glass beads. They employed the generalized wake model proposed by Bhatia and Epstein (1974) to account for bed expansion as given below:

$$\epsilon = \left[\frac{U_\ell - U_g k(1-x)}{U_e(1-\epsilon_g - k\epsilon_g)}\right]^{1/n} \{1 - \epsilon_g[1 + k(1-x)]\} + \epsilon_g[1 + k(1-x)] \tag{9}$$

where k is the ratio of the volume of the wake region to that of the bubble region in the fluidized bed, U_e is the extrapolated superficial liquid velocity as the bed voidage in the fluidized bed approaches unity, and n is the Richardson-Zaki index (Richardson and Zaki, 1954). Parameter k was empirically correlated with U_ℓ and U_g by Chern et al. (1984) as:

$$k = 0.398 U_\ell^{0.246} U_g^{-0.646} \tag{10}$$

where $2.13 \le U_g \le 26.67$ cm/s and $0.43 \le U_\ell \le 16.90$ cm/s. X is the ratio of solids holdup in the wake to that in the liquid-solid fluidized region. X is evaluated based on the empirical correlation of El-Temtamy and Epstein (1978). Gas holdup in the three-phase fluidized bed for the dispersed bubble flow regime and slug flow regime was correlated by modifying Nicklin's theory for gas-liquid bubble flow and slug flow as follows (Chern et al., 1984):

$$\frac{U_g}{\epsilon_g} = \frac{U_g}{\epsilon} + \frac{U_\ell}{\epsilon} + 10.16 + 14.88\left(\frac{U_g}{\epsilon}\right)^{1/2} \tag{11}$$

for the dispersed bubble flow regime, and

$$\frac{U_g}{\epsilon_g} = 1.783\left(\frac{U_g}{\epsilon} + \frac{U_\ell}{\epsilon}\right) + 0.35(gD_c)^{1/2} \tag{12}$$

for the slug flow regime.

The gas holdup correlation for the coalesced bubble flow regime has been correlated by Chern et al. (1984). The correlation is,

however, made with the liquid velocity less than 6.0 cm/s. Further experimental data indicate that the gas holdup increases sharply at a liquid velocity beyond 6 cm/s to the boundary of the flow regime transition to the dispersed bubble flow regime. Thus, the gas holdup for the coalesced bubble flow regime can be represented by

$$\epsilon_g = CU_\ell^{-0.98}U_g^{0.70} \tag{13}$$

where $C = 0.098$ for $2.2 \leqq U_\ell \leqq 6.0$ cm/s (Chern et al., 1984) and $C = 0.1781$ for $U_\ell > 6.0$ cm/s.

For the transition regime, the gas holdup can be approximated by an average of that calculated by Eq. 11 for the dispersed bubble flow regime and that by Eq. 12 for the slug flow regime.

Binary Mixture System

In a gas-liquid-solid fluidized bed containing a binary mixture of particles, the bed expansion and gas holdup behavior are influenced by the solids mixing states. In the complete segregation state, the fluidized bed is composed of two distinguishable parts. The upper part or flotsam region consists solely of small (or light) particles, while the lower part or jetsam region consists solely of large (or heavy) particles (except mixture X). Since each of the two regions behaves as an independent fluidized bed, hydrodynamic behavior in the flotsam region can be approximated by that in the fluidized bed of monocomponent particles. Naturally, the same approximation can be made for the jetsam region. Thus the bed expansion and gas holdup for the completely segregated binary mixture system can be treated as a linear combination of those for fluidized beds containing flotsam particles alone and jetsam particles alone. This is known as the serial model, or segregation model. From the material balances, the bed height, H, the bed voidage, ϵ, and the gas holdup, ϵ_g, can be expressed by

$$H = H_1 + H_2 = H_{10} + H_{20} \tag{14}$$

$$\epsilon = \epsilon_1 \frac{H_1}{H} + \epsilon_2 \frac{H_2}{H} \tag{15}$$

and

$$\epsilon_g = \epsilon_{g1} \frac{H_1}{H} + \epsilon_{g2} \frac{H_2}{H} \tag{16}$$

where H_{10} and H_{20} are the bed expansion heights for fluidized beds containing flotsam particles alone and jetsam particles alone, respectively. ϵ_1 and ϵ_2 are the voidages of the monocomponent bed consisting of particles 1 and 2, respectively. ϵ_{g1} and ϵ_{g2} are the gas holdups of the monocomponent bed consisting of particles 1 and 2, respectively. H_1/H and H_2/H can be expressed by

$$\frac{H_1}{H} = \frac{\dfrac{X_i}{\rho_{si}\epsilon_{si}}}{\dfrac{X_1}{\rho_{s1}\epsilon_{s1}} + \dfrac{X_2}{\rho_{s2}\epsilon_{s2}}} \tag{17}$$

The bed voidage, ϵ, and gas holdup, ϵ_g, in the fluidized bed are thus given by

$$\epsilon = \frac{\dfrac{X_1\epsilon_1}{\rho_{s1}(1-\epsilon_1)} + \dfrac{X_2\epsilon_2}{\rho_{s2}(1-\epsilon_2)}}{\dfrac{X_1}{\rho_{s1}\epsilon_{s1}} + \dfrac{X_2}{\rho_{s2}\epsilon_{s2}}} \tag{18}$$

and

$$\epsilon_g = \frac{\dfrac{X_1\epsilon_{g1}}{\rho_{s1}(1-\epsilon_1)} + \dfrac{X_2\epsilon_{g2}}{\rho_{s2}(1-\epsilon_2)}}{\dfrac{X_1}{\rho_{s1}(1-\epsilon_1)}\dfrac{X_2}{\rho_{s2}(1-\epsilon_2)}} \tag{19}$$

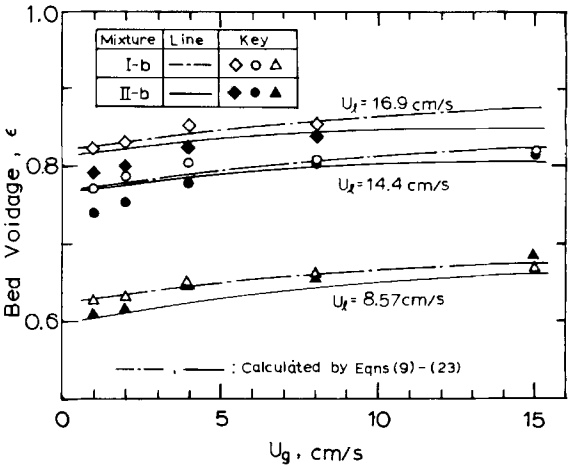

Figure 8. Bed voidage for mixtures Ib and IIb.

The values of ϵ_1 and ϵ_2 in Eqs. 18 and 19, and ϵ_{g1} and ϵ_{g2} in Eq. 19 can be readily predicted by Eqs. 9 through 13. Note that x in Eq. 9 is assumed to be zero for particles P4 through P8 (Chern et al., 1984), while the value of x for particles P1 through P3 is approximated by unity.

In the complete intermixing state, as described earlier, the hydrodynamic behavior in a gas-liquid-solid fluidized bed of a binary mixture is similar to that in a fluidized bed of uniform-property particles. Thus, the hydrodynamic behavior in the complete intermixing state for a binary mixture can be approximated by that for uniform-property particles (the property-averaging model, or aveaging model) using "characteristic" parameters of particle properties of the binary mixture system. The characteristic parameters of particle properties, $\overline{U}_e$ and $\overline{n}$, can be defined as follows to replace U_e and n, respectively, in Eq. 9 to account for the bed expansion and gas holdup in the three-phase fluidized bed of the binary mixture.

$$\overline{U}_e = \frac{X_1/\rho_{s1} + X_2/\rho_{s2}}{\dfrac{X_1}{\rho_{s1}U_{e1}} + \dfrac{X_2}{\rho_{s2}U_{e2}}} \tag{20}$$

$$\overline{n} = \frac{X_1/\rho_{s1} + X_2/\rho_{s2}}{\dfrac{X_1}{\rho_{s1}n_1} + \dfrac{X_2}{\rho_{s2}n_2}} \tag{21}$$

As will be indicated later, however, the averaging model can only be used when the bed voidage is not very large. Under a large bed voidage condition, the serial model should be used instead.

In the partial intermixing state, bed expansion and gas holdup are empirically analyzed in this study because of the difficulties involved in evaluating the degree of segregation and its effect on the bubble characteristics. The empirically obtained correlations for ϵ and ϵ_g are as follows:

$$\epsilon = 1.074\left(\frac{U_\ell}{\overline{U}_e}\right)^{0.25}\left(\frac{U_g\mu_\ell}{\sigma}\right)^{0.0172} \tag{22}$$

$$\epsilon_g = 0.182\epsilon^{1.29}\left(\frac{U_g}{U_\ell}\right)^{0.168} \tag{23}$$

The applicable ranges of U_ℓ and U_g for Eqs. 22 and 23 are limited only to those for partial intermixing state defined in the solids mixing map by Fan et al. (1984).

Figure 8 shows bed voidage plotted against gas velocity with liquid velocity as a parameter for mixtures Ib and IIb. The experimental data points cover all the solids mixing states and flow regimes. The predicted values based on the models are

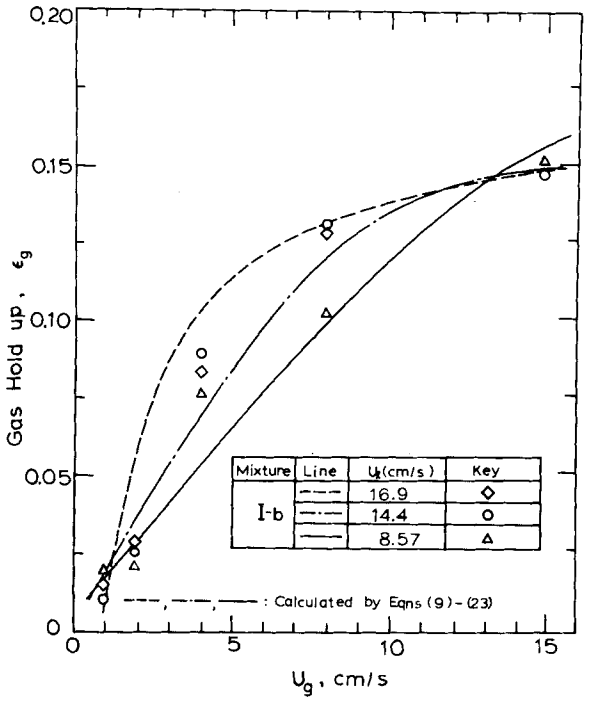

Figure 9. Gas holdup for mixture Ib.

shown by the lines in Figure 8. Good agreement is observed the predicted and experimental results.

Figures 9 and 10 show gas holdup plotted against gas velocitty with liquid velocity as a parameter for mixture Ib and IIb, respectively. The operating conditions are the same as those in Figuure 8. The predictions based on the present models are shown in the figures. It is seen that the model is reasonable at most points.

N. Epstein et al. (1981) examined the overall bed expansion in

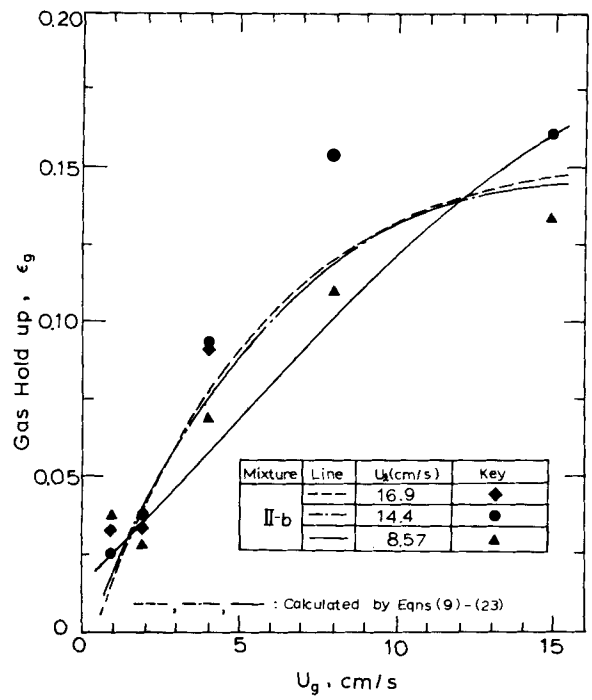

Figure 10. Gas holdup for mixture IIb.

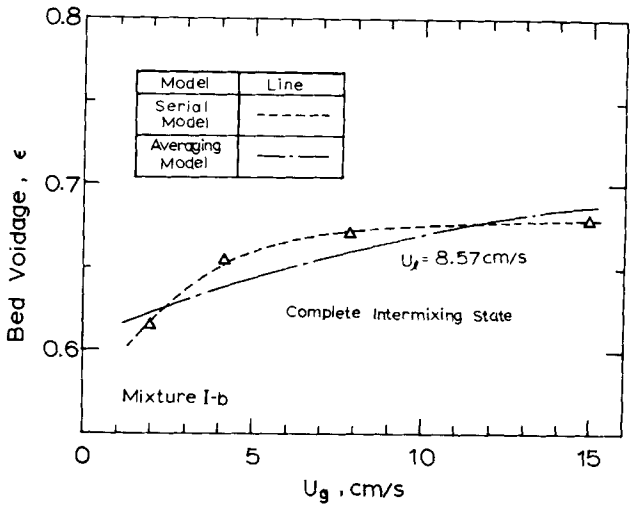

Figure 11. Comparison of bed voidage for mixture Ib obtained by experiment and by serial and averaging models.

a liquid-solid fluidized bed of binary particle mixtures. They showed that even where there is total intermixing of the two solid species, the bed expands as if it were two monocomponent beds in series. They also demonstrated the superiority of the serial model over the averaging model, and the inapplicability of relative velocity models for predicting the expansion of liquid-fluidized beds of multicomponent solids. Figure 11 compares the prediction based on the serial model with that based on the averaging model, mainly for the complete intermixing state of solids mixing for mixture Ib. It is seen from Figure 11 that the serial model follows the experimental data points much more closely than the averaging model.

As pointed out by N. Epstein et al. (1981), the serial model is a "conceptually" correct model for predicting the bed expansion for a binary mixture of particles. This is due to the fact that it predicts the correct trend of variation of bed voidage with the liquid velocity over the entire operating range of the liquid-solid fluidized bed. Even though the averaging model predicts reasonably the bed expansion at moderate liquid velocity, it fails to predict the bed expansion at high liquid velocity or large bed voidage conditions where bed voidage is dominated by the expansion of one component of the binary mixture. The serial model is particularly effective in predicting the bed expansion under high liquid velocity conditions irrespective of solids mixing states. The characteristics of the serial model reported for a liquid-solid fluidized bed (N. Epstein et al., 1981) were verified to be generally true also for a gas-liquid-solid fluidized bed in this study.

ACKNOWLEDGMENT

Acknowledgment is made to the Donor of the Petroleum Research Fund, administrated by the American Chemical Society for the partial support of this research. The valuable assistance of G. H. Song on work for Figures 8 through 11 also is acknowledged.

NOTATION

A = cross-sectional area of the column, cm^2
D_c = diameter of the column, cm
d_p = particle diameter, cm
g = gravitational acceleration, cm/s^2
H = height of the bed, cm

H_i = height of the particle i region in the complete segregation state, cm
H_{i0} = bed height for a fluidized bed containing monocomponent particle i, cm
k = ratio of the volume of the wake region to that of the bubble region
n_i = Richardson-Zaki index for particle i
n = characteristic Richardson-Zaki index for a binary mixture in the complete intermixing state
$(-dP/dz)$ = static pressure gradient, g/s²·cm²
$(-\Delta P/H)_d$ = overall dynamic pressure gradient, g/s²·cm²
$\overline{U}_e$ = extrapolated superficial liquid velocity in the liquid-solid fluidized bed as the bed voidage approaches 1; U_{ei}, for particle i, cm/s
U_e = averaged U_e, defined by Eq. 20, cm/s
U_j = superficial velocity of phase j, cm/s
$(U_\ell)_{dc}$ = superficial liquid velocity demarcating the coalesced bubble flow regime and the dispersed bubble flow regime, cm/s
U_{mf} = minimum fluidization velocity for a binary mixture system, cm/s
$(U_{mf})_M$ = minimum fluidization velocity for a fluidized bed containing monocomponent particles; $(U_{mf})_i$, for particle i; $(U_{mf})_{M0}$, at zero gas velocity, cm/s
U_t = terminal velocity of particle in liquid phase; U_{ti}, for particle i, cm/s
W_i = weight of particle i, g
X_i = weight fraction of particle i in a binary mixture
x = ratio of solids holdup in the wake to that in the liquid-solid fluidized region

Greek Letters

ϵ = bed voidage
ϵ_j = holdup of phase j
ϵ_{si} = holdup of particle i
ϵ_i = bed voidage for monocomponent system of particle i
ϵ_{gi} = gas holdup for monocomponent system of particle i
σ = surface tension of the liquid, g/s²
μ_ℓ = liquid viscosity, g/s·cm
ρ_j = density of phase j, g/cm³
ρ_s = density of particle; ρ_{si}, for particle i, g/cm³

Subscripts

1 = flotsam
g = jetsam
g = gas
ℓ = liquid
s = solid

LITERATURE CITED

Al-Dibouni, M. R., and J. Garside, "Particle Mixing and Classification in Liquid Fluidized Beds," *Trans. Inst. Chem. Eng.*, **57**, 94 (1979).

Begovich, J. M., and J. S. Watson, "Hydrodynamic Characteristics of Three-Phase Fluidized Beds," *Fluidization*, J. F. Davidson and D. L. Keains, Eds., Cambridge Univ. Press, 190 (1978).

Bhatia V. K., and N. Epstein, "Three-Phase Fluidization: A Generalized Wake Model," *Proc. Int. Symp. Fluidization and Its Applications*, H. Angelino et al., Eds., Cepadues-Editions, Toulouse, 380 (1974).

Chen, J. L. P., and D. L. Keairns, "Particle Segregation in a Fluidized Bed," *Can. J. Chem. Eng.*, **53**, 395 (1975).

———, "Particle Separation from a Fluidized Mixture, Simulation of the Westinghouse Coal Gasification Combustor/Gasifier Operation," *Ind. Eng. Chem. Proc. Des. Dev.*, **17**, 135 (1978).

Chern, S. H., L.-S. Fan, and K. Muroyama, "Hydrodynamics of Cocurrent Gas-Liquid-Solid Semifluidization with a Liquid as the Continuous Phase," *AIChE J.*, **30**, 288 (1984).

El-Temtamy, S. A., and N. Epstein, "Bubble Wake Solid Content in Three-Phase Fluidized Beds Containing Fine/Light Solids," *Int. J. Multiphase Flow*, **4**, 19 (1978).

Epstein, M. N., et al. "Incipient Stratification and Mixing in Aerated Liquid-Liquid or Liquid-Solid Mixtures," *Chem. Eng. Sci.*, **36**, 784 (1981).

Epstein, N., B. P. LeClair, and B. B. Pruden, "Liquid Fluidization of Binary Particle Mixtures. I: Overall Bed Expansion," *Chem. Eng. Sci.*, **36**, 1,803 (1981).

Epstein, N., "Hydrodynamics of Three-phase Fluidization," *Handbook of Fluids in Motion*, N. P. Cheremisinoff and R. Gupta, Eds., Ann Arbor Science, Ann Arbor, MI, 1,165 (1983).

Evstropeva, I. P., I. N. Jaganov, and P. G. Romankov, "Experimental Study of the Rates of Motion on the Phases in a Three-Phase Gas-Liquid-Solid System," *Theor. Found. Chem. Eng.*, **6**, 545 (1972).

Fan, L.-S., K. Muroyama, and S. H. Chern, "Hydrodynamics of Inverse Fluidization in Liquid-Solid and Gas-Liquid-Solid Systems," *Chem. Eng. J.*, **24**, 143 (1982).

———, "Qualitative Analysis of Solids Mixing in a Gas-Liquid-Solid Fluidized Bed Containing a Binary Mixture of Particles," *AIChE J.*, **30**, 858 (1984).

Finkelstein, E., R. Letan, and J. C. Elgin, "Mechanics of Vertical Moving Fluidized Systems with Mixed Particle Sizes," *AIChE J.*, **17**, 187 (1971).

Gibilaro, L. G., and P. N. Rowe, "A Model for a Segregation Gas Fluidized Bed," *Chem. Eng. Sci.*, **29**, 1,403 (1974).

Hoffman, R., L. Lapidus, and J. C. Elgin, "The Mechanics of Vertical Moving Fluidized Systems. IV: Application to Batch-Fluidized Systems with Mixed Particle Sizes," *AIChE J.*, **6**, 321 (1960).

Lee, J. C., A. J. Sherrard, and P. S. Buckley, "Optimum Particle Size in Three-Phase Fluidized Bed Reactors," *Proc. Int. Symp. Fluidization and Its Applications*, H. Angelino et al., Eds., Cepadues-Editions, Toulouse, 407 (1974).

Matsuura, A., and L.-S. Fan, "Distribution of Bubble Properties in a Gas-Liquid-Solid Fluidized Bed," *AIChE J.*, **30**, 894 (1984).

Mertes, T. S., and H. B. Rhodes, "Liquid-Particle Behavior. 3," *Chem. Eng. Progr.*, **51**, 517 (1955).

Moritomi, H., T. Iwase, and T. Chiba, "A Comprehensive Interpretation of Solid Layer Inversion in Liquid Fluidized Beds," *Chem. Eng. Sci.*, **37**, 1,751 (1982).

Muroyama, K., et al., "Axial Liquid Mixing in Three-Phase Fluidized Beds," *Kagaku Kogaku Ronbunshu*, **4**, 622 (1978).

Muroyama, K., and L.-S. Fan, "Fundamentals of Gas-Liquid-Solid Fluidization," *AIChE J.*, **31**, 1 (1985).

Nienow, A. W., P. N. Rowe, and L. Y. L. Cheung, "Fluidized Bed Mixing and Separation in Solid Reuse Treatment," *Powder Technol.*, **20**, 89 (1978).

Ostergaard, K., *Studies of Gas-Liquid Fluidization*, Danish Technical Press, Copenhagen, (1969).

Richardson, J. F., and W. N. Zaki, "Sedimentation and Fluidization. I," *Trans. Inst. Chem. Eng.*, **32**, 35 (1954).

Rowe, P. N., A. W. Nienow, and A. J. Agbim, "A Preliminary Quantitative Study of Particle Segregation in Gas Fluidized Beds—Binary Systems of Near Spherical Particles," *Tans. Inst. Chem. Eng.*, **50**, 324 (1972).

Sinha, V. T., M. Butensky, and D. Hyman, "Three-Phase Fluidization of Polydisperse Beads," *AIChE Symp. Ser.*, **80**, No. 241, 176 (1984).

Wen, C. Y., and Y. H. Yu, "Mechanism of Fluidization," *Chem. Eng. Prog. Symp. Ser.*, **62**, 100 (1966).

Wen, C. Y., and L.-S. Fan, "Axial Dispersion of Newtonian Liquids in Fixed and Fluidized Beds Containing Two Sizes of Particles," *J. Chinese Inst. Chem. Eng.*, **6**, 633 (1975).

Yang, W. C., and D. L. Keairns, "Rate of Particle Separation in a Gas Fluidized Bed," *Ind. Chem. Chem.*, **21**, 288 (1982).

Yoshida, K., H. Kameyama, and F. Shimizu, "Mechanism of Particle Mixing and Segregation in Gas Fluidized Beds," *Fluidization*, J. R. Grace and J. M. Matsen, Eds., Plenum, New York, 389 (1980).

Manuscript received Aug. 25, 1982; revision received Jan. 3, 1985 and accepted Jan. 8, 1985.